Effects of surface friction on a two-dimensional granular system: Numerical model of a granular collider experiment

Meenakshi Dutt and R. P. Behringer
Department of Physics, Duke University, Durham, North Carolina 27708-0305, USA
(Received 19 September 2005; revised manuscript received 25 September 2006; published 28 February 2007)

We present numerical results from a simulation of a granular collider experiment [B. Painter, M. Dutt, and R. P. Behringer, Physica D **175**, 43 (2003)] using a numerical model which accounts for substrate frictional effects [M. Dutt and R. P. Behringer, Phys. Rev. E **70**, 061304 (2004)]. We find the gradual birth and growth of a central cluster for the final state of the particles that depends on the system size, the substrate frictional dissipation, and the initial average kinetic energy. For systems where a central cluster is observed in the final state, the autocorrelation function $C(r)$ of the interparticle spacing satisfies a Gaussian functional form $C(r) = Ae^{-(r/\sigma)^2}$. We also find that the fluctuation speed distributions adhere to a Maxwell-Boltzmann distribution for times in the vicinity of collapse. Our results strongly indicate that the principal mechanism responsible for the energy and momentum dissipation is the particle-substrate kinetic friction. Our findings reiterate the importance of considering the effects of substrate friction in particle-substrate systems, as shown by the agreement between our numerical results with experimental findings of Painter, Dutt, and Behringer.

DOI: 10.1103/PhysRevE.75.021305 PACS number(s): 83.80.Fg

I. INTRODUCTION

Granular materials have been the focus of research over the past few decades due to the rich complexity of their behavior, ensuing from their ability to support the simultaneous coexistence of solid and fluid phases [1], among other reasons. The presence of substrates can greatly affect the dynamics of particles moving on them and accelerate the overall cooling of the system [2]. Studies by Painter *et al.* [2] on two particle collisions found that particles slip for an interval of time after suffering collisions with one another which resulted in an average loss of incoming energy of 63% in a single collision with a 6% contribution from restitutional effects and the remainder due to kinetic friction. The energy loss was calculated from the time of collision until the particles stopped slipping. An explanation for this behavior lies in the phenomenon of frictional frustration, which is the inability to maintain nonsliding contacts between the colliding particles and the substrate at the instant that the colliding particles are in contact with one another [2]. Effects of the substrate on the dynamics of an experimental cooling multiparticle system are discussed in Ref. [3]. Painter's results emphasized the importance of including the role of the substrate and provided deeper insight into the behavior of such systems. Numerical studies [4–7] on cooling monolayers of particles which attribute all the energy loss to restitutional effects have provided insight into the dissipative nature of these systems including clustering phenomena and granular analogs to thermodynamic quantities such as temperature and pressure. Other numerical studies [8–11] on vibrated monolayers of particles have modeled particle-substrate interactions via restitutional losses, viscous dissipation, or friction. These models have been successful in providing insight into the behavior of these driven monolayer systems such as velocity distributions and pattern formation.

In Ref. [12] we have presented numerical results for a hypothetical quasi-2D cooling granular system comprised of a monolayer of identical particles moving on a flat substrate which is bound by inelastic walls. We have used our numerical model, in which we incorporated the effects of the restitutional and substrate frictional dissipation, thereby, taking into account frictional frustration. In this work, we have applied our numerical model to simulate a 2D cooling granular experiment, namely, the granular collider experiment of Ref. [3]. The relatively high degree of correlation between the numerical and experimental results indicates the accuracy of the numerical model in depicting the effects of substrate friction on the particle dynamics, in conjunction with restitutional effects. Using realistic coefficients of rolling and kinetic friction, i.e., μ_r and μ_k, respectively, our numerical results for the time evolution of the spatial structures and the fluctuation speed distributions are in agreement with the experimental results. By correlating the fraction of the particles in the slipping state and the rate of decrease of total kinetic energy, we find that, typically, the energy loss is the highest when most of the particles are in the slipping state. On substantially reducing μ_k to values associated with μ_r, i.e., replacing kinetic friction with rolling friction, and increasing the restitutional losses to account for 63% of incoming energy loss, we find that the spatial structures no longer resemble those obtained in the experiments. Similar results are obtained when substrate friction is replaced by restitutional losses accounting for the experimentally observed 63% energy loss.

The structure of this paper is as follows. Section II provides a synopsis of the granular collider experiment and the numerical simulation. Section III presents the numerical results with emphasis on spatial structures, speed distributions, energy dissipation, and effects of reducing/neglecting substrate friction. Section IV summarizes this paper with some discussions and conclusions.

II. THE GRANULAR COLLIDER EXPERIMENT AND THE NUMERICAL EXPERIMENT

A schematic diagram along with the details of the experiment can be found in Ref. [3]. The experiment was designed

to allow the particles (3.18 mm diameter steel spheres) to simultaneously roll down a conic section-shaped rubber incline onto a circular black anodized aluminum substrate of radius 12.72 cm. This setup allows the particles to gain kinetic energy in a controlled fashion (via the height of the incline) as they roll down the slope and onto the aluminum substrate, where they collide among each other, losing energy and momentum and finally coming to rest. A typical final state consists of a central cluster containing the majority of the particles, with some additional outliers. When the particles begin moving on the aluminum substrate, the experiment becomes a cooling granular system comprised of particles dissipating energy and momentum due to collisional and substrate frictional losses. An example of the tracks of the particles for the entire duration of an experimental run with 150 particles can be found in Ref. [3].

The model considered here links the collisional dynamics with the substrate friction [12] in order to provide a numerical simulation that captures the salient features of the granular collider experiment. In the numerical experiment, we assume our system to have a circular geometry where the particles are moving on a substrate, emulating the aluminum plate. The dimensions of the particles and the aluminum plate are identical to those used in the experiment. The system is not bound, enabling a particle to leave the system altogether. For the initial conditions, we assume the particles have rolled down the rubber incline and therefore, place them in concentric rings at a radius corresponding to the bottom edge of this incline. To each particle, we assign an appropriate radially inward velocity (based on the height of the incline) on which is superposed small random fluctuations. Once the initial conditions are set, the particle dynamics are determined by our numerical model. We use a hard-sphere event-drive molecular dynamics algorithm as the computational framework for the numerical experiment. There are two types of interactions which can take place: (1) interparticle collisions and (2) substrate interactions due to rolling and slipping friction. From an algorithmic perspective, these two types of interactions define two types of computational events: interparticle collisions and the slipping of a particle between a collision and its return to the state of pure rolling. At each iteration, a computation of all possible future events is calculated, and the one occurring in the shortest time interval is chosen as the next event. The type of frictional forces and torques experienced by a particle will depend upon its state of motion: pure rolling or slipping. In addition to substrate frictional losses, the particles experience restitutional dissipation [4]. Additional details of the model appear both in the Appendix and in Ref. [12].

III. NUMERICAL RESULTS

We have explored the behavior of various system sizes with different initial average kinetic energies and degrees of dissipation. However, in this paper, we present results for a 500 particle system with $\mu_r=0.0025$, $\mu_k=0.4$, and height $=0.38$ cm using velocity dependent coefficients of restitution [12], unless specified otherwise.

A. Spatial distributions

At the onset of the simulation, all the particles have a dominant radial velocity component which enables the particles to move radially inwards to the center of the plate, simultaneously suffering many collisions. During the process of these multiple collisions, the particles lose energy and momentum due to restitutional and substrate frictional losses; each collision is followed by a slipping phase for both the participating particles. Kinetic friction, apart from being highly dissipative, is also responsible for curving the trajectories of the particles, leading to interesting spatial patterns; with rolling friction, it also guarantees that all particles come to rest in a finite amount of time. The temporal evolution of the spatial pattern during a typical simulation run is shown in Fig. 1. On average, the particles move radially inwards towards the center of the substrate resulting in a collapse. The multiple collisions suffered by the particles during their inward motion sustain the thermal component of the particle's velocity, which, nevertheless, remains small compared to the dominant radial velocity component. After collapse, a large fraction of the particles remain trapped in the central cluster, with only a few particles escaping the system, or moving to the periphery of the central cluster. As the formation of the central cluster occurs, particles trapped there have many more nearest and next-nearest neighbors, as compared to those in the periphery, resulting in multiple collisions which randomize the directions, although not so much the magnitudes, of their velocities. Particles in the periphery may scatter from the cluster or simply remain in the periphery.

The various factors which influence the evolution of the spatial configuration are the number of particles used in the numerical experiment, the coefficient of substrate friction, and the incoming kinetic energy of the particles, as set by the height of the incline (h, with the initial average particle speed v given by $v=\sqrt{2hg}$ where g is the acceleration due to gravity). With increasing numbers of particles in the system, the final system state evolves from particles scattered all over the substrate to particles grouped in a single large central cluster (with very few particles or small-sized clusters at the periphery). The effects of substrate friction and the incline height for a given number of particles are summarized in Fig. 2. Changes in these quantities have the expected effects. Higher values of μ_k increase the substrate frictional dissipation suffered by a particle after a collision, and lead to increased confinement of particles in the central cluster or a fewer number of particles leaving the cluster. Increasing the initial average kinetic energy allows the particles in the periphery of the central cluster to rebound, or scatter away from the cluster, overcoming the frictional dissipation and eventually leaving the system.

The number of particles in the numerical experiment strongly influences the formation of the central cluster, which is the dominant final feature. However, if the particle number is too small, the cluster is weak or nonexistent. Simulations for 150 particles ($\mu_r=0.0025$, $\mu_k=0.232$, 0.4) and 100 particles ($\mu_r=0.0025$, $\mu_k=0.4$) show some weak signs of a final cluster. However, simulation for the 100 particle system ($\mu_r=0.0025$, $\mu_k=0.232$) did not show a strong cluster, and indeed, was characterized by rolling motion of free particles

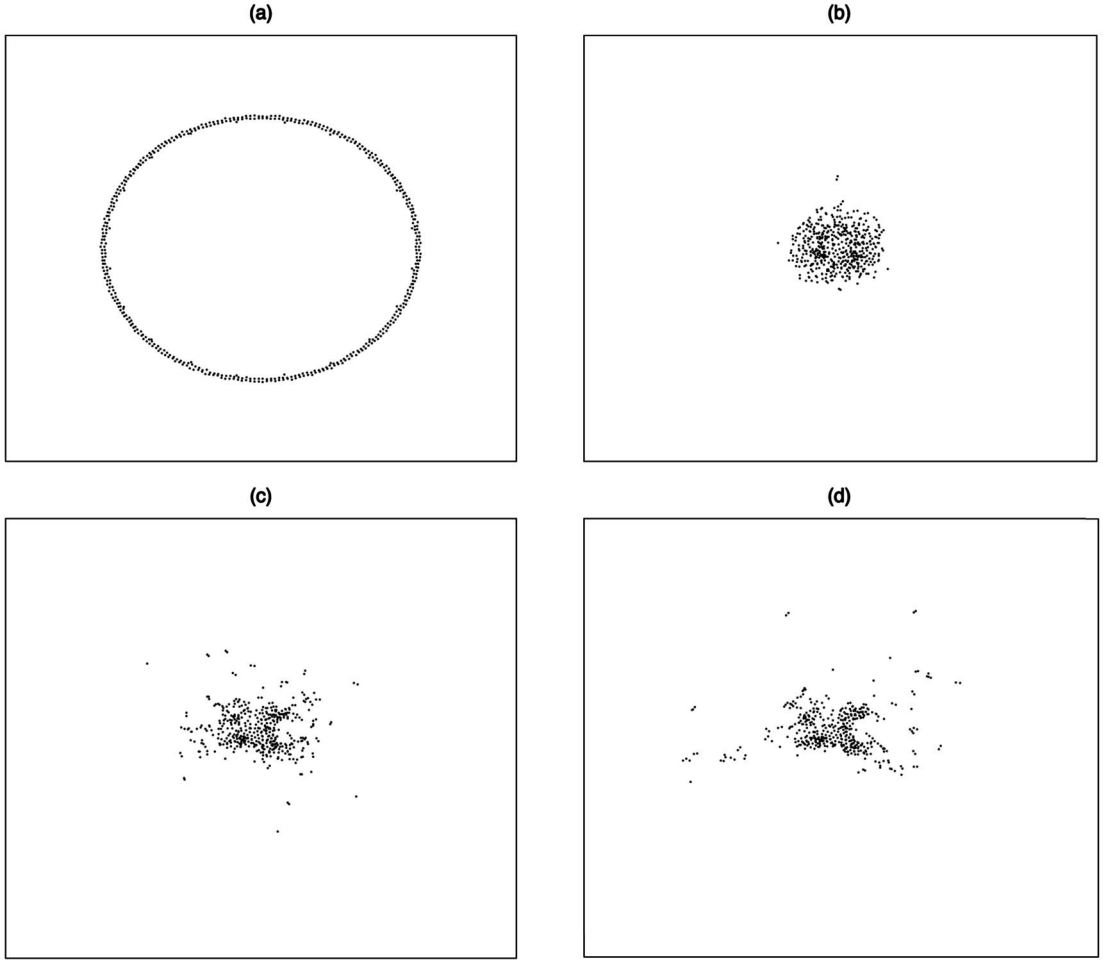

FIG. 1. Spatial configurations of the particles for times (a) $t=0.0$ s, (b) $t=0.38$ s, at collapse (c) $t=0.78$ s, (d) $t=3.75$ s, the simulation has stopped.

when the simulation was terminated. The radial and number density profiles of the final spatial configuration, as shown in Figs. 3 and 4, summarize the strength of clusters as a function of the system size and kinetic friction.

An important feature is the spatial structure associated with the formation of the cluster. Insight into this issue can be obtained by looking at variations of the particle positions about the center, and by the autocorrelation of the interparticle positions. Figure 5 plots δr, the root mean square distance (r.m.s.) from the center of mass (c.m.) of the system in the final state, as a function of time for 200, 400, 600, and 700 particles. The common theme for the various system sizes is the monotonic decrease in δr with time until δr reaches a minimum (at the point of collapse). After collapse, an interesting rebound effect is observed as the central cluster shows an effective dilation due to the particles trapped in the cluster recoiling after impact. With increasing number of particles in the system, the change in δr after collapse decreases. The decrease in the fluctuation about the c.m. with an increase in the number of particles emphasizes that the dilation of the cluster has an inverse dependence on the number of particles. Similarly, the time at which collapse occurs is dependent upon the number of particles in the system, the substrate friction, and the height of the incline. Figure 6 plots

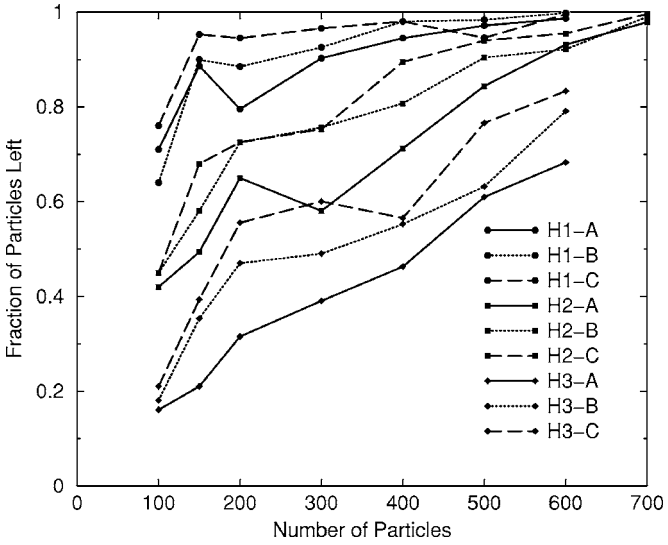

FIG. 2. Fraction of the particles remaining in the system once the simulation stops as a function of the number of particles used in the numerical experiments. H1: height=0.381 cm, H2: height =0.762 cm, H3: height=1.524 cm. A: $\mu_r=0.0025$, $\mu_k=0.232$; B: $\mu_r=0.0025$, $\mu_k=0.3$; C: $\mu_r=0.0025$, $\mu_k=0.4$.

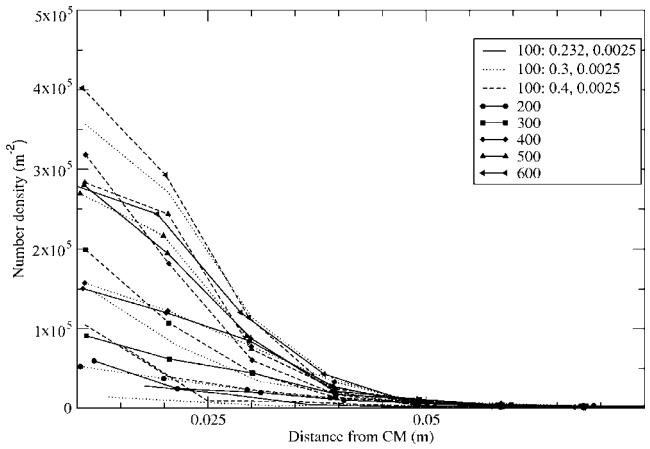

FIG. 3. Radial density profile for the final spatial configurations of simulations carried out with different number of particles and values of μ_k and μ_r, as indicated, in the legend.

the time of collapse, i.e., the time interval between the commencement of the simulation and the r.m.s. distance about the c.m. attaining a minimum value, as a function of the number of particles at different values of μ_k and the height of the incline. The time to collapse for low initial average kinetic energy grows gradually with increasing values of μ_k and the number of particles.

The time evolution of the spatial correlations of the particles in the system provides a quantitative measure of the behavior as a function of the number of particles, the coefficients of friction, and the initial average kinetic energy. The spatial correlation is quantified by the spatial autocorrelation function $c(\vec{r})=\int \rho(\vec{x})\rho(\vec{x}-\vec{r})d\vec{x}$, where $\rho(\vec{x})$ is the density of particles, which is calculated by summing over delta functions at the particle centers. $c(\vec{r})$ is then averaged over all angles and normalized by the number of particles in the system N to give $C(r)$. The autocorrelation function $C(r)$ gives the distribution of particles in the system relative to each other and is extremely useful in providing insight into the formation of coherent spatial structures. Figure 7 shows how

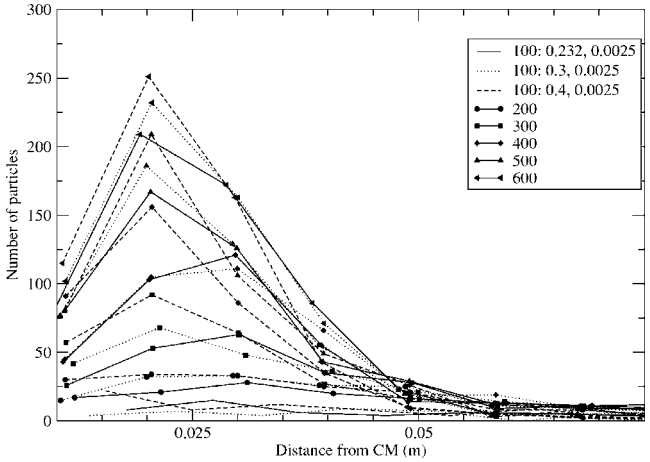

FIG. 4. Radial number profile for the final spatial configurations of simulations carried out with different number of particles and values of μ_k and μ_r, as indicated, in the legend.

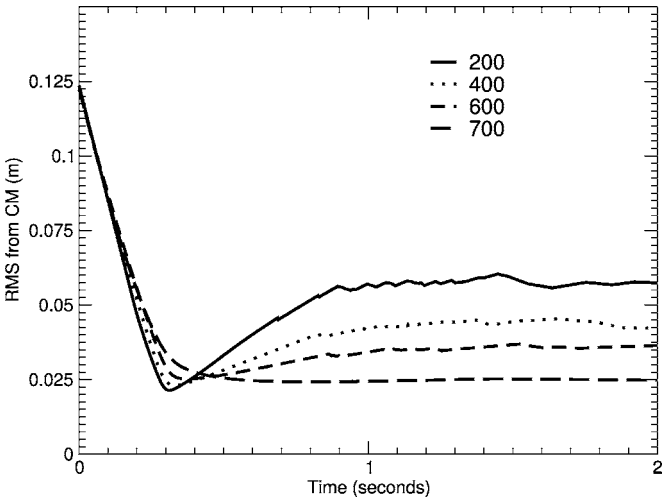

FIG. 5. The r.m.s. fluctuation about the center of mass position of the particles for 200, 400, 600, and 700 particles with μ_r =0.0025, μ_k=0.4.

the spatial correlations evolve with time, with each curve representing the spatial autocorrelation function $C(r)$ at a given instant. At t=0 s, there are two peaks: one peak occurring at a large r ($r\sim$76–78), and the other occurring at a lower r ($r\sim$1–2). The latter represents contributions from the nearest neighbor distances, and the former represents particles that are diametrically opposite to one another (separated by the diameter of the plate)—see Fig. 1(a). As time progresses, the outer peak (the peak occurring at a large r) occurs at decreasing values of r until $C(r)$ reduces to a single peaked structure. This is a manifestation of the particles moving towards the center of the plate in a coherent manner until they suffer collapse in the center of the substrate. After the initial collapse, the functional form of $C(r)$ with time

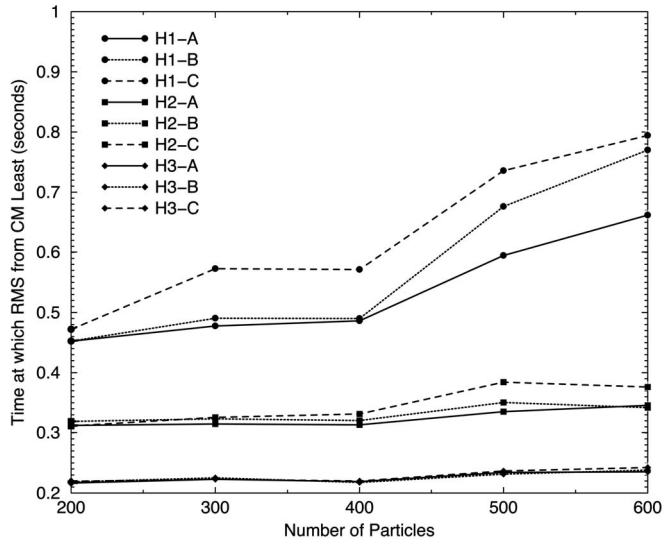

FIG. 6. A plot of the time at which the r.m.s fluctuation about the center of mass position is at a minimum as a function of the number of particles. H1: height=0.381 cm, H2: height=0.762 cm, H3: height=1.524 cm. A: μ_r=0.0025, μ_k=0.232; B: μ_r=0.0025, μ_k=0.3; C: μ_r=0.0025, μ_k=0.4.

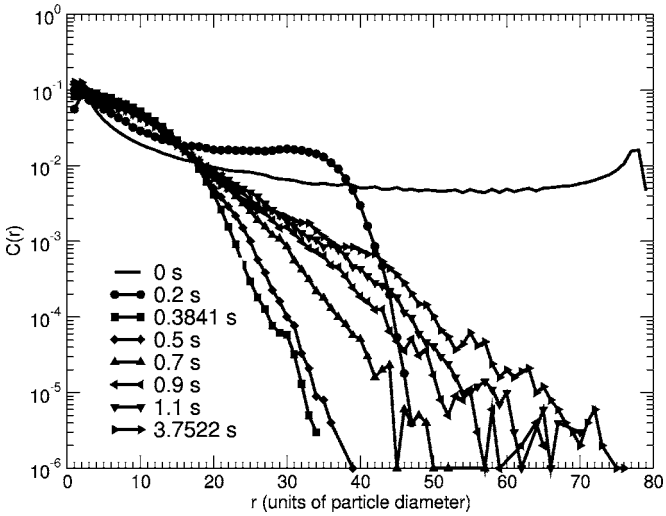

FIG. 7. A plot of the autocorrelation function $C(r)$ vs interparticle distance in the units of particle diameter at different instances of a simulation, for 500 particles.

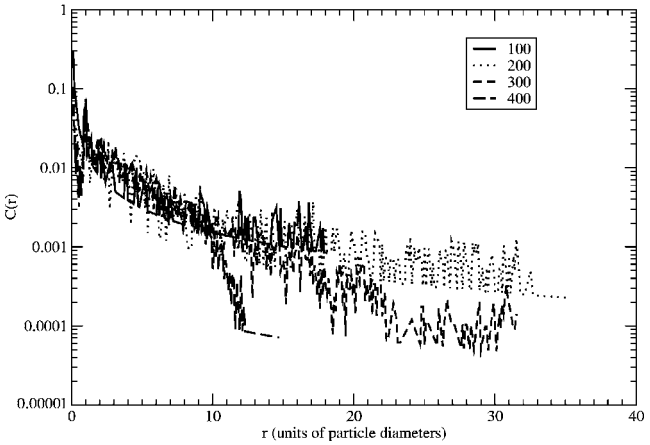

FIG. 8. A plot of the autocorrelation function $C(r)$ vs interparticle distance in the units of particle diameter at the final spatial configuration for simulations carried out with different number of particles N (as shown in the legend). The friction coefficients for $N \geq 100$ are all $\mu_k = 0.4$ and $\mu_r = 0.0025$. For $N = 100$ and $N = 200$, $C(r)$ is overlapping [up to $r \simeq 18$, where $C(r)$ stops for $N = 100$].

depends on the initial number of particles in the system, the coefficients of friction and, the height of the incline. With increasing initial number of particles, $C(r)$ remains invariant until a certain value of r ($\sim$17–18)—let us call this r_c—beyond which $C(r)$ tends to spread out with time prior to the simulation coming to a halt. This behavior can be explained by considering the overall particle dynamics after collapse. Once collapse occurs, the central cluster traps a very large number of particles which suffer rapid collisions among themselves—losing energy and momentum. Thus, there is very little change in the position of the particles trapped in the cluster in the interval commencing from the time of collapse to the end of the simulation, accounting for $C(r)$ remaining essentially invariant for the regime $r \leqslant r_c$. However, the few particles that managed to escape the central cluster account for the spreading out of $C(r)$ in the tail $r > r_c$. In general, we have found the spatial autocorrelation function $C(r)$ for the final states of a wide range of system sizes approximately adheres to an exponential functional form $C(r) = Ae^{(-br)}$ for smaller system sizes as opposed to the Gaussian functional form $C(r) = Ae^{-(r/\sigma)^2}$ for larger systems. Figure 8 summarizes the evolution of the spatial autocorrelation function $C(r)$, for the final states, with various system sizes. The transition in the functional form of $C(r)$ occurs for a system size between 200 and 300 particles.

Figure 9 plots the location of the $C(r)$ peak occurring at the higher value of r as a function of time, for time intervals spanning the beginning of the simulation to shortly before $C(r)$ becomes a single peaked function. Each set of points in Fig. 9 is for a different value of the initial average kinetic energy. For a given initial average kinetic energy, the velocity of the $C(r)$ peak, given by the slope of each set of points, is almost constant, and is found to be almost independent of the number of particles. Before the double peaked structure in $C(r)$ disappears, the particles in their annular arrangement move coherently, i.e., almost as in a single composite structure. This is a manifestation of the initial conditions imposing a dominant radial velocity component to each particle, with minimal slipping. As one might expect, the slope of each set of points decreases with the incline height. Table I compares the ratios of the slopes of the curves in Fig. 9 to the initial average speed for a given height. The ratio has an approximately constant value of 2 for the various incline heights. Thus, the annular structure is composed of particles which are moving diametrically towards one another and which maintain a speed that is approximately that of the initial average particle speed.

B. Speed distributions

Cooling granular materials exhibit speed distributions which evolve with time in a manner that depends upon many

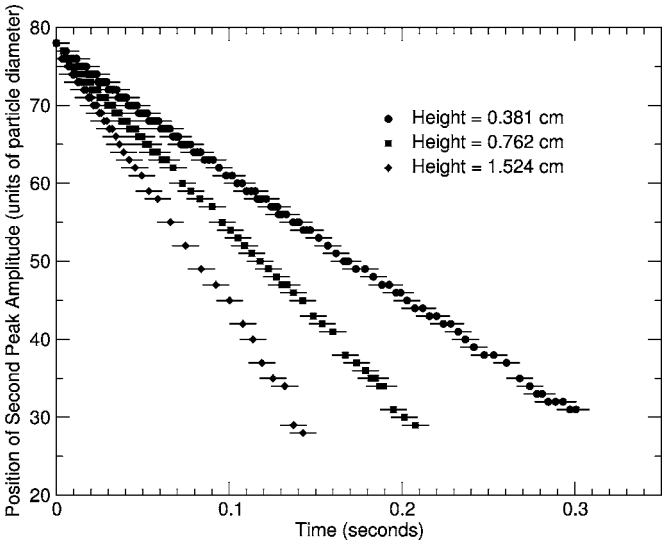

FIG. 9. The position of the peak amplitude of the spatial autocorrelation function $C(r)$ (at the higher interparticle distance) as a function of time.

TABLE I. Comparison of the ratio of the slope (m) of the data sets for each height (h) in Fig. 9 normalized by the average initial speed for the given height; d is the particle diameter (=3.18 mm).

h (cm)	Slope m (d/s)	$v_0=(2gh)^{1/2}$ (m/s)	m/v_0
0.381	−157.4736	0.2734	1.8316
0.762	−233.9034	0.3866	1.9237
1.524	−342.6594	0.5468	1.9927

aspects, including the initial conditions of the system in question. Speed distribution measurements are useful indicators of departures from molecular chaos. Particles in our system typically cannot be treated as a thermodynamic gas [whose speed fluctuations $\vec{u}=\vec{v}-\langle\vec{v}\rangle$ satisfies the Maxwell-Boltzmann (MB) distribution in 2D $P(u)=Aue^{-Bu^2}$] due to the spatial inhomogeneity and correlations in the particle velocities. Although each simulation begins with a MB distribution, the material is unable to maintain that distribution over a prolonged period of time, due to the high rate of energy and momentum dissipation (made significantly higher by the presence of a substrate).

We plot representative distributions at different instances of a numerical experiment for which collapse occurs at $t=0.384$ s in Fig. 10. For early times, $t\sim0.1226$ to ~0.2137 s [Figs. 10(a) and 10(b)], most of the particles have mean fluctuation speeds ~30 cm/s due to the dominant radially inward flow, with an initial speed of 38.66 cm/s. As the particles collide, their velocities become increasingly randomized to the extent that the fluctuation speeds fit a MB distribution. For times close to but before collapse, the fluctuation speed distribution continues to approximate a MB distribution. After the collapse, the fraction of particles in the lower speed/fluctuation speed range grows dramatically, and the distribution ceases to be even approximately MB. This is demonstrated by the exponential fit that the fluctuation speeds satisfy at $t=0.7201$ s. Eventually, all the particles will come to rest in a finite time.

C. Energy dissipation

On account of the difference in energy dissipation for rolling vs slipping particles, it is useful to consider the populations of these two states, as compared to the rate of kinetic energy dissipation. Figure 11 compares the fraction of particles in the slipping state and the rate of decrease of total kinetic energy as a function of time. From 0.03 s onward, these two quantities shadow each other. For earlier times, dissipation exceeds slipping fraction (on the indicated scales) implying that collisional losses must be dominant. Interestingly, there is a time interval from ~0.03 to ~0.2 s when dissipation and slipping are declining. This lull is terminated dramatically by the event at $t\simeq0.3$ s. The peak that occurs for $t\sim0.3$–0.4 s is after collapse when all the particles are trapped in or close to the central cluster, and are suffering numerous collisions. At other times when the fraction of particles in the slipping state is less than 0.5, the energy and momentum losses are dominated by rolling friction and collisions. This indicates that kinetic friction is responsible for a large fraction of the energy and momentum dissipation in these systems, as further highlighted in Sec. III D.

D. Effects of significantly reducing substrate friction

An interesting query concerns the consequences of significantly reducing or removing substrate friction, or replac-

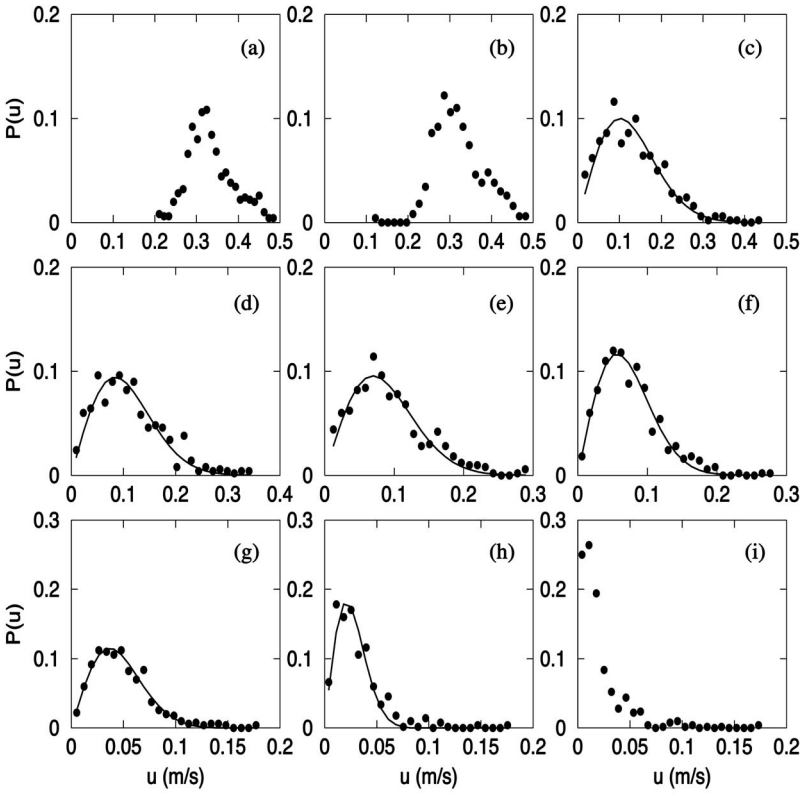

FIG. 10. Fluctuation speed distributions $P(u)$ vs u at times (a) $t=0.1226$ s, (b) $t=0.2137$ s, (c) $t=0.3525$ s, (d) $t=0.3623$ s, (e) $t=0.3719$ s, (f) $t=0.3841$ s collapse, (g) $t=0.4210$ s, (h) $t=0.5251$ s, (i) $t=0.7201$ s. The dots represent the numerical data points; the lines in (c)–(h) have been fitted to the MB distribution: and the line in (i) has been fitted to an exponential. [Note the change of scales for $P(u)$ in the bottom row. The initial inward speed was 38.66 cm/s.]

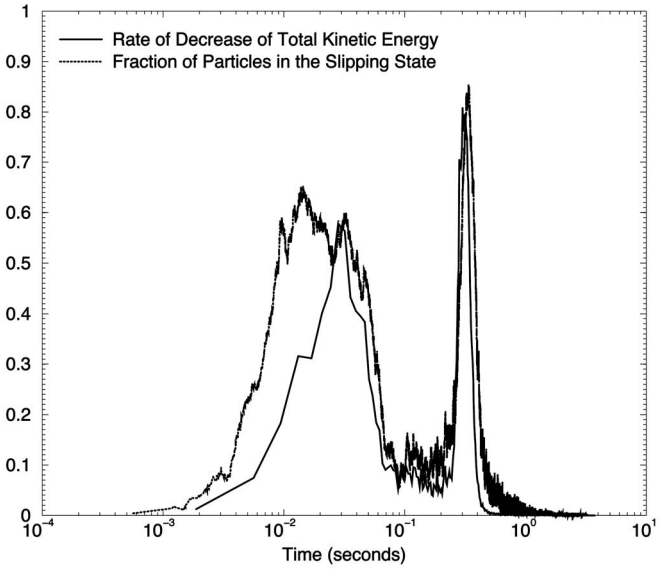

FIG. 11. A plot of the fraction of particles left in the slipping state and the rate of decrease of total kinetic energy as a function of time. The rate of energy decrease has been scaled by the maximum value.

ing dissipation by substrate friction with the appropriate restitutional coefficients which would lead to realistic percentages of energy losses (which Painter *et al.* [3] found to be about 63%). Figure 12 shows the final spatial states for four systems, each consisting of 500 particles with different frictional and restitutional coefficients. Figure 12(a) gives simulation results for $\mu_r=\mu_k=0.0025$ with realistic velocity-dependent restitution coefficients; Fig. 12(b) gives results for $\mu_r=\mu_k=0.0025$ with restitution coefficients which accounted for 63% energy loss at a collision; Fig. 12(c) gives results for zero substrate friction with velocity dependent restitution coefficients and Fig. 12(d) with zero substrate friction with restitution coefficients which allowed for 63% energy loss. The objective of the simulation for Fig. 12(d) is to simulate the effect of only restitutional losses that are as large as would occur on average in the presence of realistic kinetic friction. We find that all the particles escape from the system as the collisional and frictional losses are not sufficient to confine all the particles in the central cluster after collapse. By using the same small values of μ_r and μ_k but restitution coefficients which allowed energy loss of 63%, the confinement or clustering increases due to the higher restitutional losses, and the larger linear and angular velocity changes which result in longer slipping times. However, the confinement of the particles is not as effective as for those simulations using realistic values of μ_r and μ_k, and velocity-dependent coefficients of restitution. Thus, removal of substrate friction or lessening of kinetic friction reduces particle confinement significantly.

The obvious effect of reducing the friction ($\mu_r=\mu_k=0.0025$) while using velocity dependent restitutional coefficients is that most of the energy loss comes from restitutional losses and not substrate frictional losses as demonstrated in Fig. 13. Figure 13 is a plot of the average collision rate (normalized by the maximum value), fraction of the particles in the slipping state, and rate of decrease of total kinetic energy as a function of time for a 500 particle system. Even though the fraction of particles in the slipping state remains at a high value for a prolonged period of time (on

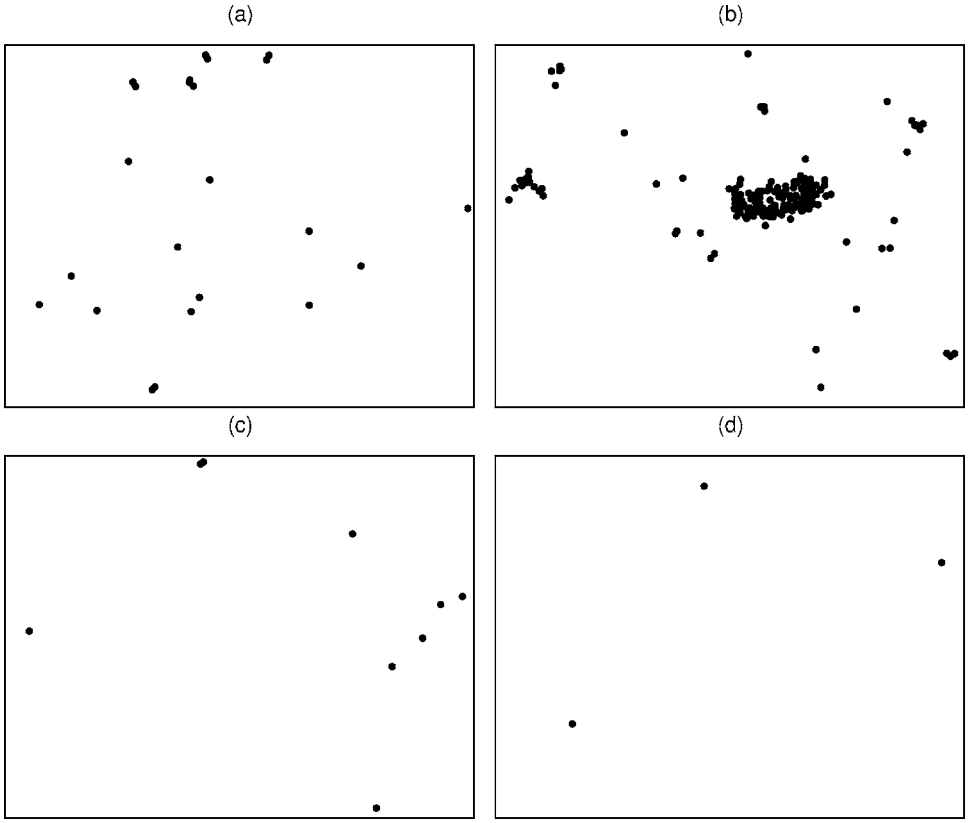

FIG. 12. Final spatial configurations for simulations using 500 particles with (a) $\mu_r=0.0025$, $\mu_k=0.0025$ and velocity dependent restitution coefficients; (b) $\mu_r=0.0025$, $\mu_k=0.0025$ and restitution coefficients which account for 63% energy loss; (c) $\mu_r=0.0$, $\mu_k=0.0$ and velocity dependent restitution coefficients; and (d) $\mu_r=0.0$, $\mu_k=0.0$, restitution coefficients which account for 63% energy loss.

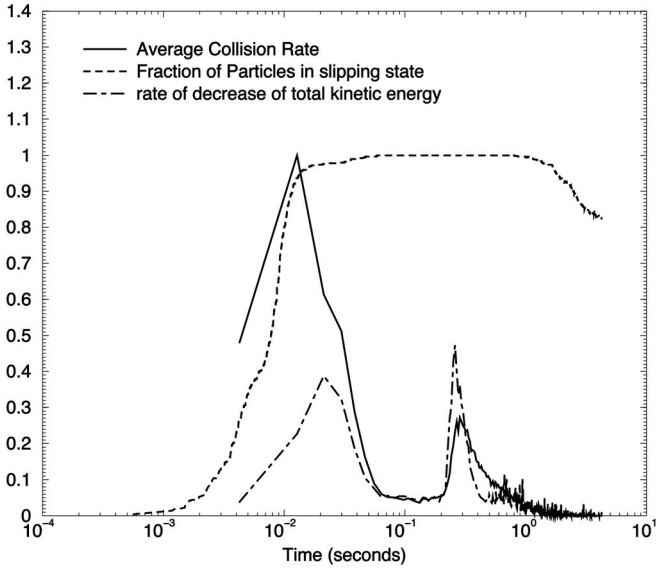

FIG. 13. The time evolution of the average collision rate, the fraction of the particles in the slipping state, and the rate of decrease of total kinetic energy for a 500 particle system with μ_r=0.0025, μ_k=0.0025 and velocity dependent coefficients of restitution.

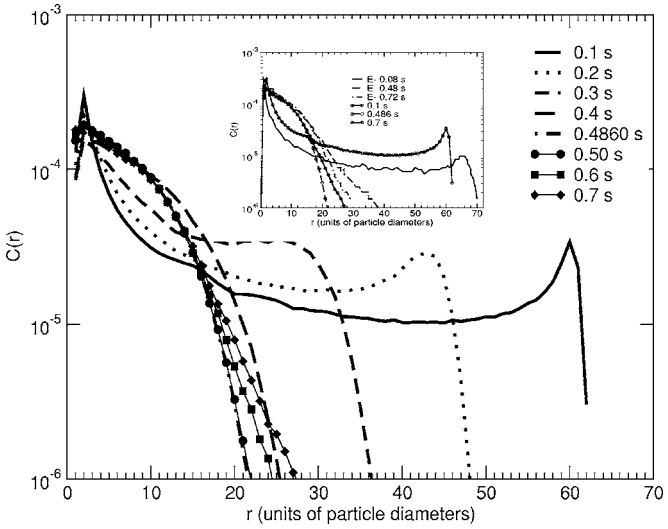

FIG. 14. The spatial autocorrelation function $C(r)$ for a system of 400 particles at different instances of a single numerical realization (μ_r=0.0025, μ_k=0.232 and height=0.381 cm). The inset shows $C(r)$ as a function of the radial distance r (particle diameters) for a single realization of the experimental and numerical runs using 400 particles. The numerical simulation has been carried out using μ_r=0.0025, μ_k=0.232 and height=0.381 cm. The experimental data is from Painter and is indicated by the E.

account of the low value of μ_k and hence, longer slipping times), the peaks in the rate of decrease of total kinetic energy coincide with those for the average collision rate.

IV. DISCUSSION AND CONCLUSIONS

A. Comparison to experiments

A comparison between the numerical and experimental results provides insight into the physical accuracy of the numerical model. One point for comparison is the variation in the final spatial states with the system size. Here we consider Fig. 1–4 vs Fig. 7 from Ref. [3]; both show similar trends of decreasing fractions of particles escaping the central cluster with increasing cluster size. We have also found agreement in the evolution of the spatial structures in both the simulations and experiments. Figure 14 shows the time evolution of the autocorrelation function $C(r)$ for a single realization of a numerical simulation using a 400 particle system. (The numerical simulation for the 400 particle system used the following parameters: μ_r=0.0025, μ_k=0.232 and height =0.38 cm.) Figure 14 can be compared to an analogous single experimental realization using 400 particles (Fig. 8 of Ref. [3]). Since the normalization of the two data sets differs, we appropriately rescale the numerical results and we find that the two calculations show reasonably good agreement. We also find qualitative agreement in the time evolution of the fluctuation speed distributions for a 400 particle system (Fig. 28 in Ref. [3] and Fig. 10). Certainly, the agreement between our numerical results and the experimental results depends strongly on the inclusion of realistic values of μ_k.

B. Conclusions

In this paper we have presented results from our numerical simulations of the cooling granular experiment [3]. These simulations use a numerical model which allows us to link the details of the restitutional and substrate frictional effects on a multiparticle-substrate system [12].

We find that this system exhibits interesting spatial structures, in particular the formation of a dense central cluster, with increasing particle number, with increasing coefficient of kinetic friction μ_k, and more weakly, with decreasing height of the incline. These changes affect both clustering and the fraction of particles left in the system at the end of the simulation. We find that the fluctuation speed distributions of the system fit a MB distribution indicating that the particles undergo thermalization shortly before and after collapse; subsequently, the fluctuation speed distributions become decaying exponential functions as a significant fraction of the particles in the clusters have cooled but the particles in the periphery of the clusters are still energetic. For realistic frictional values, the rate of energy loss is the highest when most of the particles in the system are in the slipping state, which is one of the indicators of the highly dissipative nature of kinetic friction. When μ_k is reduced to 0.0025 (=μ_r), most of the particles escape the system after collapse; however, by introducing high restitutional losses some clustering is observed.

In summary, these results underscore the importance of including the effects of substrate friction to properly understand the behavior of multiparticle-substrate systems. It is equally important to be able to link the phenomena of substrate friction to the restitutional dynamics in the system. The general framework of this model can used to study other multiparticle-substrate systems.

ACKNOWLEDGMENT

This work has received support from NSF Grant Nos. DMR-0137119 and DMR-0555431.

APPENDIX

The two special cases for the binary collision rule for two spherical particles i and j with different masses ($m_i \neq m_j$) of radii a, positions $\vec{r}_i$ and $\vec{r}_j$, linear velocities $\vec{v}_i$ and $\vec{v}_j$, and angular velocities $\vec{\omega}_i$ and $\vec{\omega}_j$, respectively, is given as follows. (1) For collisions of two particles, i and j with identical masses, i.e., $m_i = m_j$, the collision rule is [15]

$$\vec{v}_i' = \vec{v}_i - \frac{1+\alpha}{2}\vec{v}_n - \frac{q}{2}\frac{1+\beta}{1+q}(\vec{v}_t + \vec{v}_r), \tag{A1}$$

$$\vec{v}_j' = \vec{v}_j + \frac{1+\alpha}{2}\vec{v}_n + \frac{q}{2}\frac{1+\beta}{1+q}(\vec{v}_t + \vec{v}_r), \tag{A2}$$

$$a\vec{\omega}_i' = a\vec{\omega}_i + \frac{1+\beta}{2(1+q)}\hat{n} \times (\vec{v}_t + \vec{v}_r), \tag{A3}$$

$$a\vec{\omega}_j' = a\vec{\omega}_j + \frac{1+\beta}{2(1+q)}\hat{n} \times (\vec{v}_t + \vec{v}_r). \tag{A4}$$

(2) For particle-wall collisions (as walls are infinitely massive), i.e., $m_j \gg m_i$

$$\vec{v}_i' = \vec{v}_i - (1+\alpha)\vec{v}_n - q\frac{1+\beta}{1+q}(\vec{v}_t + \vec{v}_r), \tag{A5}$$

$$\vec{v}_j' = 0, \tag{A6}$$

$$a\vec{\omega}_i' = a\vec{\omega}_i + \frac{1+\beta}{1+q}\hat{n} \times (\vec{v}_t + \vec{v}_r), \tag{A7}$$

$$a\vec{\omega}_j' = 0, \tag{A8}$$

where

$$\vec{v}_c = \vec{v}_i - \vec{v}_j - a(\vec{\omega}_i + \vec{\omega}_j) \times \hat{n},$$

$$\hat{n} = \frac{r_i - r_j}{|r_i - r_j|},$$

$$\vec{v}_c' \cdot \hat{n} = -\alpha \vec{v}_c \cdot \hat{n},$$

$$\vec{v}_c' \times \hat{n} = -\beta \vec{v}_c \times \hat{n},$$

$$\vec{v}_n = \hat{n}(\vec{v}_i - \vec{v}_j) \cdot \hat{n},$$

$$\vec{v}_t = \vec{v}_i - \vec{v}_j - \vec{v}_n,$$

$$\vec{v}_r = -a(\vec{\omega}_i + \vec{\omega}_j) \times \hat{n},$$

$$\vec{v}_c = \vec{v}_n + \vec{v}_t + \vec{v}_r.$$

For particle-wall collisions, the normal unit vector $\hat{n}$ is the unit vector perpendicular to the wall surface pointing from the contact point with the wall to the center of the particle. We attach a coefficient "p" or "w" for particle-particle or particle-wall collisions. Further details can be found in Refs. [13–16].

[1] H. M. Jaeger, S. R. Nagel, and R. P. Behringer, Rev. Mod. Phys. **68**, 1259 (1996).
[2] B. Painter and R. P. Behringer, Phys. Rev. E **62**, 2380 (2000).
[3] B. Painter, M. Dutt, and R. P. Behringer, Physica D **175**, 43 (2003).
[4] S. McNamara and S. Luding, Phys. Rev. E **58**, 813 (1998).
[5] S. Luding and H. J. Hermann, Chaos **9**, 673 (1999).
[6] I. Goldhirsch, Chaos **9**, 659 (1999).
[7] I. Goldhirsch, M.-L. Tan, and G. Zanetti, J. Sci. Comput. **8**, 1 (1993).
[8] A. Prevost, D. A. Egolf, and J. S. Urbach, Phys. Rev. Lett. **89**, 084301 (2002).
[9] J. S. van Zon, J. Kreft, D. I. Goldman, D. Miracle, J. B. Swift, and H. L. Swinney, Phys. Rev. E **70**, 040301(R) (2004).
[10] M. P. Ciamarra, A. Coniglio, and M. Nicodemi, Phys. Rev. Lett. **94**, 188001 (2005).
[11] X. Nie, E. Ben-naim, and S. Y. Chen, Europhys. Lett. **51**, 679 (2000).
[12] M. Dutt and R. P. Behringer, Phys. Rev. E **70**, 061304 (2004).
[13] D. E. Wolf, in *Computational Physics Selected Methods—Simple Exercises—Serious Applications*, edited by K. H. Hoffmann and M. Schreiber (Springer, Heidelberg, 1996).
[14] S. Luding, Phys. Rev. E **52**, 4442 (1995).
[15] S. Luding, *Physics of Dry Granular Media*, edited by H. J. Herrmann, J.-P. Hovi, and S. Luding (Kluwer Academic Publishers, Dordrecht, 1998), p. 285.
[16] G. Kuwabara and K. Kono, Jpn. J. Appl. Phys., Part 1 **26**, 1230 (1987).